Available online at www.sciencedirect.com

SciVerse ScienceDirect

Ceramics International 39 (2013) 877–881

CERAMICS INTERNATIONAL

www.elsevier.com/locate/ceramint

Short communication

Fabrication of a ZrC–SiC matrix for ceramic matrix composites via in-situ reaction and its application

Qinggang Li[a,b,c], Shaoming Dong[a,b,*], Zhen Wang[a,b], Jianbao Hu[a,b,c], Bin Wu[a,b,c], Haijun Zhou[a,b], Ping He[a,b], Jinshan Yang[a,b,c]

[a] *State Key Laboratory of High Performance Ceramics and Superfine Microstructure, Shanghai Institute of Ceramics, Chinese Academy of Sciences, Shanghai 200050, China*
[b] *Structural Ceramics and Composites Engineering Research Center, Shanghai Institute of Ceramics, Chinese Academy of Sciences, Shanghai 200050, China*
[c] *Graduate University of Chinese Academy of Sciences, Beijing 100049, China*

Received 3 April 2012; received in revised form 8 June 2012; accepted 8 June 2012

Abstract

A ZrC–SiC matrix was fabricated by means of in-situ reaction method, by using zirconium powders, silicon powders and phenolic resin as raw materials. The crystal size and morphology of the synthesized matrix were characterized by scanning electron microscopy. The microstructures, as well as mechanical and ablative properties of three-dimensional C_f/ZrC–SiC composites were studied. The flexural strength of the composite was 257 MPa, and the elastic modulus was 59.3 GPa. The anti-ablation property was evaluated via a plasma wind tunnel test. Results show that the shape and surface of the composite remains intact, being the composite almost unabated.

Keywords: A. In-situ reaction; B. Composites; E. Application; ZrC–SiC matrix

1. Introduction

Ultra-high-temperature ceramics are a class of materials with extremely high melting temperatures, such as diborides and carbides of zirconium and hafnium. They are of particular interest because of their unique combination of properties such as, besides the highest refractoriness, high electrical and thermal conductivity, chemical inertness against molten metals or nonbasic slag and superb thermal shock resistance [1]. These properties make them attractive candidates for high-temperature applications, aerospace, and leading-edge parts on hypersonic re-entry space vehicles, where resistance to corrosion, wear and oxidation is demanded [1–3].

Carbon fiber reinforced silicon carbide matrix (C_f/SiC) composites are widely used in high temperature structural elements for aerospace equipments, such as rocket nozzles, nosetip, aeronautic jet engines, and leading edges, because of its unique physicochemical and mechanical properties [4–7]. However, the use of traditional silicon carbide matrix composites is limited because of the oxidation of silicon carbide, which is disadvantageous to ultra-high-temperature oxidation [8–9]. To improve the high-temperature performance of C_f/SiC composites, new materials are required in advanced thermal protection system. Thus, refractory carbides such as zirconium carbide (ZrC) need to be introduced into the SiC matrix in the composites to fabricate carbon fiber reinforced ultra-high-temperature (C_f/UHTCs) matrix composites [8]. ZrC has gained much attention due to its exceptional properties, including a high melting point (up to 3540 °C), and the ability to form refractory oxide scales at high temperatures. ZrC also has a relatively low density (6.7 g/cm^3) that is half of that of HfC (12.2 g/cm^3) [10]. ZrC is one of the most promising ceramics for ultrahigh temperature applications due to the high melting point (2700 °C) of its protective zirconia (ZrO_2) layer.

---

[*] Corresponding author at: State Key Laboratory of High Performance Ceramics and Superfine Microstructure, Shanghai Institute of Ceramics, Chinese Academy of Sciences, Shanghai 200050, China.
E-mail address: smdong@mail.sic.ac.cn (S. Dong).

0272-8842/$36.00
http://dx.doi.org/10.1016/j.ceramint.2012.06.030

The introduced methods of ZrC phase are various. In our previous study, a liquid precursor conversion method using ZrC precursor and polycarbosilane (PCS) was used to fabricate C_f/ZrC–SiC composites [8,9]. Given that processing conditions are critical to the successful synthesis of ZrC–SiC mixed matrices, the selection of pyrolysis temperature and microstructures of the matrices were studied. Other techniques have been utilized to introduce ZrC into C_f/SiC composites to improve their high temperature properties. Wang et al. fabricated C_f/UHTCs composites using hot-pressing and polymer infiltration pyrolysis (PIP) [11], as well as mold-pressing and polymer infiltration and pyrolysis (PIP) [12]. Other methods include chemical vapor infiltration (CVI) combined with modified polymer infiltration pyrolysis (PIP) [13], a soft-solution approach using inorganic precursors [11]. However, some of these processes have obvious disadvantages, such as long fabrication period, higher cost and difficult reproducibility.

So the purpose of this work is how to synthesize simply and rapidly a ZrC–SiC matrix via in-situ reaction using Zr powders, Si powders and thermosetting phenolic resin as raw materials. The effects of pyrolysis temperature on the matrix fabrication process and microstructures were studied. Meanwhile, the mechanical and ablation properties of the obtained C_f/ZrC–SiC composites fabricated through in-situ reaction were also investigated.

2. Experimental procedure

Carbon fibers (T300SC, Toray, Tokyo, Japan) with an average diameter of 6 μm were used. The three-dimensional (3D) fabrics were fabricated by the Nanjing Fiberglass Research and Design Institute (Nanjing, China). The architecture had a fiber distribution of 8:2:1 in the *x:y:z* directions, respectively, and ~40% fiber volume fraction. The experimental procedure for the preparation of a ZrC–SiC matrix is described as follows. First, zirconium (Zr) powder (<43 μm, >98 wt% pure, High Purity Chemical, Saitama, Japan), silicon (Si) powder (<10 μm, 99.9 wt% pure, High Purity Chemical, Saitama, Japan), and thermosetting phenolic resin (Shanghai Qinan Adhesive Material Factory, Shanghai, China) were first ball milled at an appropriate volume ratio by ultrasonic agitation to form a homogenously dispersed slurry using ethyl alcohol as solvent.

For XRD analysis it was then cured using a rotating evaporator. Thermosetting phenolic resin solution was applied as the carbon resource. The cured mixtures were pyrolyzed at 900 °C in an argon atmosphere at a rate of 10 °C/min. Afterwards, the pyrolytic products were ground into powder and sieved through a metallic sieve (mesh size = 250 μm). This process is only for XRD analysis. The pyrolytic products were heat treated in a graphite crucible using a high-temperature graphite resistance furnace in the range of 1400–1700 °C in an argon atmosphere at a rate of 10 °C/min.

To manufacture the 3D C_f/ZrC–SiC composites, the performs (10 mm × 80 mm × 100 mm) were first coated with PyC/SiC interphase (~200 nm) by forced pressure-pulsed chemical vapor infiltration (FP-CVI). After this process, the slurry of Zr powder, Si powder, thermosetting phenolic resin, and ethyl alcohol was infiltrated into the fiber perform, cured and pyrolysed under the same conditions. The obtained composites were further densified via seven cycles of PIP process, and then heated at 1650 °C in a high-temperature graphite resistance furnace at a rate of 10 °C/min to open the closed pores. The in-situ reaction was accompanied by a heat-treatment process. During the in-situ reaction, Zr powders and Si powders were allowed to react with the carbon from the pyrolysis of thermosetting phenolic resin to form ZrC and SiC, respectively.

The phase compositions of the powdered pyrolytic product were characterized by X-ray diffraction (XRD) with Cu K_α radiation. The microstructures of the composites were studied by Electron Probe Micro-analyzer (EPMA, JXA-800, Jeol, Tokyo, Japan). The crystalline size and morphology of the synthesized matrix were characterized by scanning electron microscopy (SEM).

The 3-D C_f/ZrC–SiC composites were cut and ground into 5 mm × 4 mm × 60 mm specimen for three-point-bending tests in an Instron-5566 machine, operated at a crosshead speed of 0.5 mm/min and a span of 48 mm. Both the polished cross sections and the fracture surfaces were observed by Electron Probe Micro-analyzer (EPMA, JXA-800, Jeol, Tokyo, Japan).

The anti-ablation test was performed in a plasma wind tunnel environment, with approximately 25120 ± 2512 kW/m^2 heat flux and 2400 K flame temperature. Nitrogen pressure was 0.5 MPa, whereas the gas flow rate was 13596 l/h. The arc voltage and arc current were 185 ± 5 V and 550 ± 10 A, respectively, whereas the pressure of cool water and heater power were 1.5 MPa and approximately 100 kW, respectively. The nozzle diameter and electrode distance were 8 mm and 3.3 mm to 4.0 mm, respectively. During the test, the specimen with a size of 80 mm × 80 mm × 10 mm was vertically exposed to the flame for 600 s when the surface temperature of the composite reached 2400 K. The distance between the nozzle tip and the surface of the specimen was 10 ± 0.2 mm and the flame ablation angle was 90°. The surface temperature of the sample was monitored using an optical pyrometer.

3. Results and Discussions

3.1. Matrix material characterization

Fig. 1 shows the XRD patterns of the matrix samples obtained by pyrolyzing the slurry of Zr powders, Si powders, and thermosetting phenolic resin at 900 °C for 30 min and 1650 °C for 60 min. After holding at 900 °C for 30 min, XRD diffraction identified ZrO_2 and Si phases. The presence of oxygen is caused by traces of it in argon and creates traces of ZrO_2. However, after heating at 1650 °C for 60 min, the ZrO_2 peaks disappear, indicating the completion of ZrO_2 conversion into ZrC, and the SiC phase is confirmed. Thus, a pure ZrC–SiC matrix can be obtained at 1650 °C for 60 min.

The SEM and TEM images of the ZrC–SiC matrix heated at 1650 °C for 60 min are shown in Fig. 2. From the SEM images, the particle sizes of the matrix range between 200 and 400 nm, with a nearly spherical morphology. However, agglomeration still exists. In addition, SiC whiskers are formed during the in-situ reaction process. Based on the TEM images, it is shown that the ZrC phases (dark background in the backscattered electron micrograph) are regularly dispersed in the SiC matrix (white background).

3.2. Composite material properties

The XRD patterns of the composite are plotted in Fig. 3 at different temperatures. At 1200 °C, the main phases existing in the composite are ZrC and ZrO_2, and the SiC phase is not found. It indicates that the carbothermal reactions are not completed at 1200 °C. There is insufficient available temperature to reduce ZrO_2 into ZrC. However, it can be concluded that from the diffraction peaks after 1650 °C that the main phases are ZrC and SiC. This finding implies that the ZrC and SiC are formed through in-situ reaction from Zr powders, Si powders, and thermosetting phenolic resin as raw materials at 1650 °C.

The SEM micrographs of the polished cross-section of the 3-D C_f/ZrC–SiC composite are shown in Fig. 4. For the composites fabricated by in-situ reaction, it can be seen that there are still a few pores in the composite (Fig. 4a). The mixture slurry prefers to fill large pores between the fiber bundles. The generated ZrC and SiC are dense and seal the pores inside the composites. The distribution of ZrC and SiC are uneven, which is caused by the pore distribution in carbon fiber porous perform. Based on Fig. 4b, a coating is formed on the surface of the fibers, and the matrices exhibit a core–shell encapsulation structure. EDAX conducted on the interphase layer detects that the coating on the surface of the fibers is ZrC coating, and the shell of the core–shell encapsulation structure is ZrC, and the core is a mixture of ZrC and SiC. In the in-situ reaction process, the C atoms from the thermosetting phenolic resin diffuse into the Zr and Si sites and form the ZrC and SiC in situ, respectively.

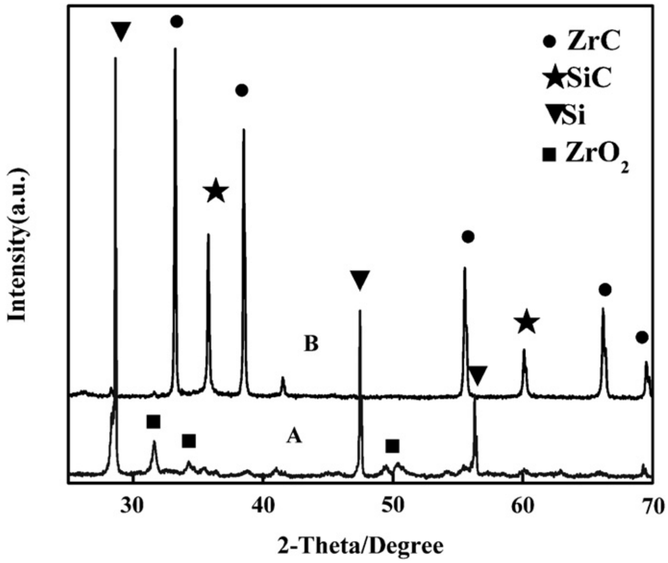

Fig. 1. XRD patterns of the ZrC–SiC matrix: (A) at 900 °C for 30 min and (B) at 1650 °C for 60 min.

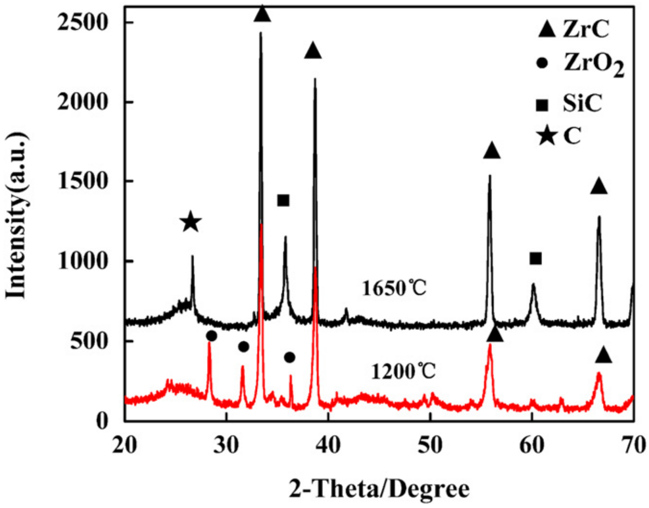

Fig. 3. XRD patterns of 3-D C_f/ZrC–SiC composite.

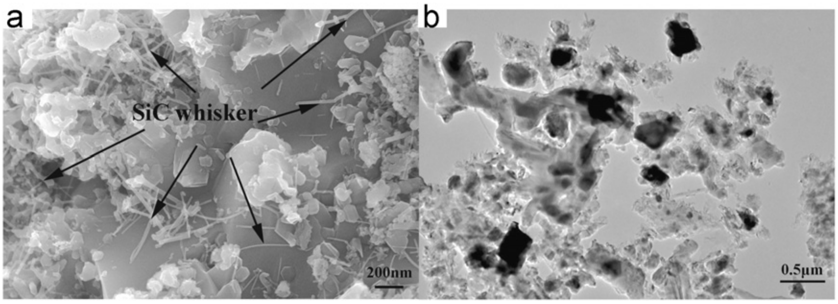

Fig. 2. SEM and TEM images of the ZrC–SiC matrix at 1650 °C for 60 min: (a). SEM image and (b). TEM image.

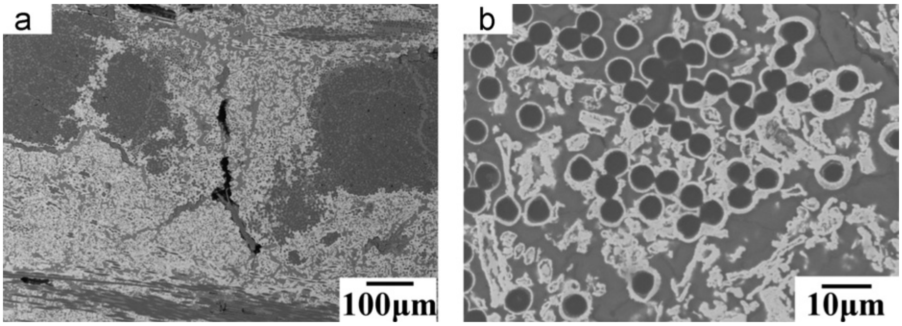

Fig. 4. Back-scattered electron images for the polished cross-sections of 3-D C_f/ZrC–SiC composite: (a), back-scattered electron image and (b), larger magnification.

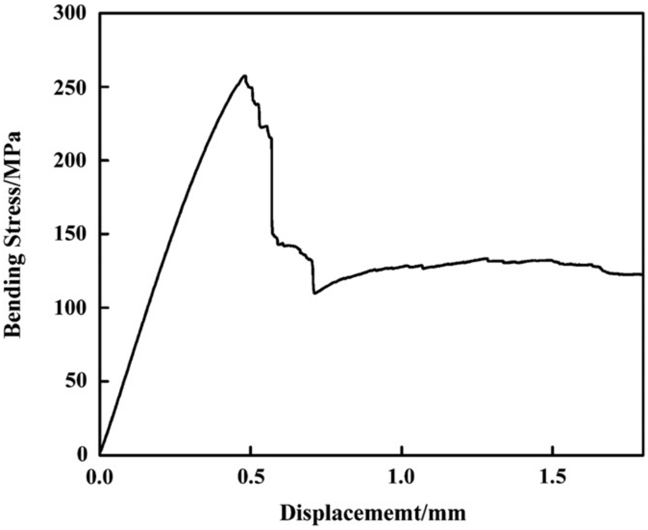

Fig. 5. Bending stress/displacement curves of 3-D C_f/ZrC–SiC composite.

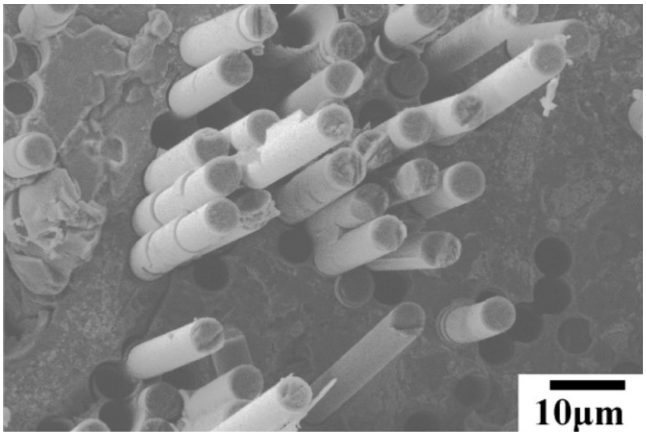

Fig. 6. SEM micrograph on the fracture surfaces of 3-D C_f/ZrC–SiC composite.

Fig. 5 shows the bending stress–displacement curve of the 3-D C_f/ZrC–SiC composite with PyC/SiC interphase deposited. It can be concluded from the curve that the sample shows a typical non-brittle fracture behavior. The 3-D C_f/ZrC–SiC composite has a bending strength of 257 ± 21 MPa, and the elastic modulus is of 59.3 ± 11 GPa.

The morphologies of the fracture surfaces are shown in Fig. 6. It can be seen that the composite shows a typical non-brittle fracture behavior and there are fiber pullouts accompanying the fracture process. It can also be observed that the pulled-out fibers are long and their surfaces are smooth. When PyC/SiC interphase is deposited, weak bonding between the fibers and the matrix occurs. Consequently, deflection and fiber pulling-out, which benefit to the improvement of fracture toughness, are facilitated.

The high-temperature property of the C_f/UHTC composite is important: hence, the 3-D C_f/ZrC–SiC composite was evaluated via a plasma wind tunnel test. Fig. 7 shows the morphologies of the 3-D C_f/ZrC–SiC composite before (Fig. 7a), and after (Fig. 7c) the plasma wind tunnel test. The mass loss and the linear recession rates are 0.0012 g/s and -0.0003 mm/s. Using the obtained morphologies on the composite surface before and after the plasma wind tunnel test, it can be seen that the shape and surface of the composite remain intact, and that the composite is almost without ablation. As a results, the 3-D C_f/ZrC–SiC composite excellent anti-ablation properties.

4. Conclusions

In conclusion, a ZrC–SiC matrix was fabricated by means of in-situ reaction, using zirconium powders, silicon powders and phenolic resin and their pyrolysis at 1650 °C for 60 min. The ZrC–SiC matrix had a small average crystalline size (<400 nm). However, agglomeration still exists. In addition, SiC whiskers are formed during the in-situ reaction process. Finally, 3-D C_f/SiC–ZrC composites were successfully fabricated by in-situ reaction process. The sample shows a typical non-brittle fracture behavior. The 3-D C_f/ZrC–SiC composite has a bending strength of 257 MPa, and the elastic modulus is of 59.3 GPa. To qualify the composites for the application on the high temperature, the plasma wind tunnel test is necessary and very interesting. During the plasma wind tunnel test the mass loss rate of the composite was 0.0012 g/s, and the liner recession rate was -0.0003 mm/s. The fabricated 3-D C_f/SiC–ZrC composites had anti-ablative properties. The

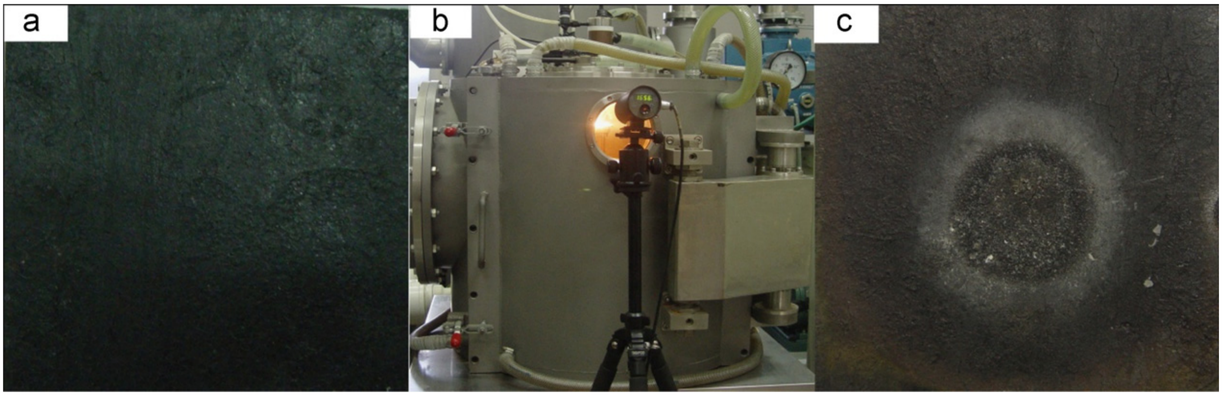

Fig. 7. The plasma wind tunnel test of 3-D C_f/ZrC–SiC composite: (a) before ablation, (b) in the middle of ablation and (c) after ablation.

further study of the good performance of the fiber-pull-out would be continued.

Acknowledgments

Authors appreciate the financial support of the National Natural Science Foundation of China under the Grant no. of 51172256 and the Innovation Program of Shanghai Institute of Ceramics Chinese Academy of Sciences under the Grant no. of Y12ZC6160G. Authors also thank Professor Xiaolei Wu and Professor Heji Huang from the Institute of Mechanics Chinese Academy of Sciences for the plasma wind tunnel test.

References

[1] K. Upadhya, J.M. Yang, W.P. Hoffmann, Materials for ultrahigh temperature structural applications, American Ceramic Society Bulletin 76 (12) (1997) 51–56.

[2] S.R. Levine, E.J. Opila, M.C. Halbig, J.D. Kiser, M. Singh, J.A. Salem, Evaluation of ultra-high temperature ceramics for aeropropulsion use, Journal of the European Ceramic Society 22 (2002) 2757–2767.

[3] M.M. Opeka, I.G. Talmy, E.J. Wuchina, J.A. Zaykoski, S.J. Causey, Mechanical, thermal, and oxidation properties of refractory hafnium and zirconium compounds, Journal of the European Ceramic Society 19 (1999) 2405–2414.

[4] T.M. Besmann, B.W. Sheldon, R.A. Lowden, D.P. Stinton, Vapor phase fabrication and properties of continuous filament ceramic composites, Science 253 (1991) 1104–1109.

[5] R. Naslain, A. Guette, F. Rebillat, R. Pailler, F. Langlais, X. Bourrat, Boron-bearing species in ceramic matrix composites for long-term aerospace applications, Journal of Solid State Chemistry 177 (2004) 449–456.

[6] S. Schmidt, S. Beyer, H. Knabe, H. Immich, R. Meistring, A. Gessler, Advanced ceramic matrix composite materials for current and future propulsion technology applications, Acta Astronautica 55 (2004) 409–420.

[7] W. Krenkel, B. Heidenreich, R. Renz, C/C–SiC composites for advanced friction systems, Advanced Engineering Materials 4 (2002) 427–436.

[8] Q.G. Li, H.J. Zhou, S.M. Dong, Z. Wang, P. He, J.S. Yang, B. Wu, J.B. Hu, Fabrication of a ZrC–SiC matrix for ceramic matrix composites and its properties, Ceramics International (2012) 023, http://dx.doi.org/10.1016/j.ceramint.2012.01.

[9] Q.G. Li, S.M. Dong, Z. Wang, P. He, H.J. Zhou, J.S. Yang, B. Wu, J.B. Hu, Fabrication and properties of 3-D C_f/SiC–ZrC Composites, using ZrC precursor and polycarbosilane, Journal of the American Ceramic Society 95 (4) (2012) 1216–1219.

[10] R. Naslain, R. Pailler, X. Bourrat, D. Bertarnd, L. Lamouroux, Synthesis of highly tailored ceramic matrix composites by pressure-pulsed CVI, Solid State Ionics. (2001) 541–548.

[11] Z. Wang, S.M. Dong, X.Y. Zhang, H.J. Zhou, D.X. Wu, Q. Zhou, D.L. Jiang, Fabrication and properties of C_f/SiC–ZrC composites, Journal of the American Ceramic Society 91[10] (2008) 3434–3436.

[12] Z. Wang, S.M. Dong, Y.S. Ding, X.Y. Zhang, H.J. Zhou, J.S. Yang, B. Lu, Mechanical properties and microstructures of C_f/SiC–ZrC composites using T700SC carbon fibers as reinforcements, Ceramics International 37 (2011) 695–700.

[13] N. Padmavathi, S. Kumari, V.V.B. Prasad, J. Subrahmanyam, K.K. Ray, Processing of carbon-fiber reinforced (SiC+ZrC) mini-composites by soft-solution approach and characterization, Ceramics International 35 (2009) 3447–3454.